

1 **On the potential for regolith control of fluvial terrace**
2 **formation in semi-arid escarpments**

3
4 **Kevin P. Norton¹, Fritz Schlunegger², Camille Litty²**

5
6 [1]{School of Geography, Environment and Earth Sciences, Victoria University of
7 Wellington, New Zealand}

8 [2]{Institute of Geological Sciences, University of Bern, Switzerland}

9 Correspondence to: K.P. Norton (kevin.norton@vuw.ac.nz)

10
11 **Abstract**

12 Cut-fill terraces occur throughout the western Andes where they have been associated with
13 pluvial episodes on the Altiplano. The mechanism relating increased rainfall to sedimentation
14 is however not well understood. Here, we apply a hillslope sediment model and reported
15 cosmogenic nuclide concentrations in terraces to examine terrace formation in semi-arid
16 escarpment environments. We focus on the Rio Pisco system in western Peru in order to
17 determine probable hillslope processes and sediment transport conditions during phases of
18 terrace formation. Specifically, we model steady state and transient hillslope responses to
19 increased precipitation rates. The measured terrace distribution and reconstructed sediment
20 loads measured for the Rio Pisco agree with the transient model predictions, suggesting strong
21 climatic control on the cut-fill sequences in western Peru primarily through large variations in
22 sediment load. Our model suggests that the ultimate control for these terraces is the
23 availability of sediment on the hillslopes with hillslope stripping supplying large sediment
24 loads early in wet periods. At the Rio Pisco, this is manifest as an approximately 4x increase
25 in erosion rates during pluvial periods. We suggest that this mechanism may also control
26 terrace occurrence in other semi-arid escarpment settings.

1 **1 Introduction**

2 High elevation plateaus are commonly associated with either passive margins (e.g. Africa, Sri
3 Lanka, Australia) or large convergent mountain systems (e.g. Himalaya, Andes). In either
4 case, erosion on the plateau edge leads to the formation of rapidly eroding escarpments
5 adjacent to the more slowly eroding plateaus (*Kober et al.*, 2006; *Matmon et al.*, 2002; *Seidl*
6 *et al.*, 1996; *van der Beek et al.*, 2002; *Vanacker et al.*, 2007; *von Blanckenburg et al.*, 2004;
7 *Weissel and Seidl*, 1997). In this paper, we suggest that weathering is a dominant control on
8 river form in escarpment settings as it is responsible for the production of sediment through
9 the formation of regolith. The antiquity of most of these plateaus suggests that they erode
10 through parallel retreat (*Schlunegger et al.*, 2006) with somewhat constant topographic
11 profiles. These large topographic gradients often result in orographic precipitation on the
12 escarpment (e.g. *Bookhagen and Strecker*, 2008). Since chemical weathering is at least
13 partially dependent on water supply (e.g. *White and Blum*, 1995a), regolith formation is also
14 likely to be enhanced on the plateau, especially during wet phases.

15 Quaternary climate change has led to fluctuations in the available precipitation on both the
16 plateaus and adjacent valleys. The fluvial cut and fill terrace systems, which are common in
17 these settings, are typically attributed to this climate variability (*Bookhagen et al.*, 2006;
18 *Steffen et al.*, 2009). Using a climate-dependent regolith production algorithm (*Norton et al.*,
19 2014) coupled with simple sediment transport laws (e.g. *Tucker and Slingerland*, 1997), we
20 investigate the effects of climate change in the form of precipitation variation on the hillslope
21 system and propose that hillslope regolith production and stripping may control cut and fill
22 sequences during the Late Quaternary.

23

24 **2 Setting**

25 We focus on the Rio Pisco drainage basin, situated on the western Andean margin at c. 17° S,
26 central Peru. This stream flows from its headwaters at ~4000 m asl across the Altiplano
27 Plateau before plunging into a deeply incised canyon. This region marks a broad knickzone,
28 which connects the mostly non-incised Miocene Altiplano Plateau to the flat, low-lying
29 coastal plains (Figure 1). The high elevation plateau is characterized by high precipitation
30 rates and low erosion rates, while the knickzone exhibits lower precipitation rates but much
31 faster erosion (Figure 2). The knickzone is interpreted to maintain its slope while eroding
32 headward due to low erosion rates at the plateau margin (*Abbühl et al.*, 2011). Above the

1 knickzones, the streams are still graded to the Miocene baselevel. This high elevation plateau
2 could be the result of dynamic reorganization of river channels (*Willett et al.*, 2014) and/or the
3 uplift of the western Andes (e.g. *Schlunegger et al.*, 2006, *Schildgen et al.*, 2007). Along the
4 knickzone, the Rio Pisco is currently under sediment capacity as evidenced by the narrow
5 modern channel where the stream cuts into valley fill and bedrock. The upper river reaches
6 are primarily bedrock channels, while lower reaches are alluvial. Downstream of the
7 knickzone, the floodplain widens and the river becomes braided, attesting to an excess of
8 sediment.

9 A series of cut-fill terraces and debris flow deposits fill the widening channel to within ~40km
10 from the coast (e.g. *Steffen et al.*, 2009; *Bekaddour et al.*, 2014). These valley fills consist of
11 both fluvial conglomerates and hillslope-derived debris flow breccias, which could indicate
12 phases of landsliding (e.g. *McPhillips et al.*, 2014). We proceeded according to *Litty et al.*
13 (2015) and measured the exposed thickness and extent of >100 terraces in the Pisco Valley
14 (Figure 3). These were classified as fluvial (composed of moderately-well sorted, well-
15 rounded clast-supported cobbles) or colluvial (composed of poorly sorted, angular to sub-
16 rounded, matrix-supported clasts; Figure 4). The terraces were correlated based on elevation
17 and composition.

18 *Steffen et al.* (2009) dated the Late Quaternary terraces, which are abundant in the lower
19 reaches downstream of the knickzone, from ~40 to 120 km downstream distance. The ages of
20 the terrace accumulation correspond with well-known wet periods in the western Andes (e.g.
21 Minchin, 47.8-36 ka and Tauca, 26-14.9 ka, *Baker et al.*, 2001a, 2001b; *Fritz et al.*, 2004;
22 *Placzek et al.*, 2006). As documented by *Steffen et al.* [2009], regolith is shed over ca. 10-15
23 ka timescales from the hillslopes as debris flows during these pluvial periods. These authors
24 suggested that increased rainfall resulted in increased erosion and thereby increased sediment
25 supply to the river, causing a phase of deposition in the valley, starting generally with debris
26 flows from the hillslopes. They argued that as hillslopes became depleted of sediment, the
27 river begins to incise again while discharge remains high. While this scenario is logical, the
28 ability of sediment delivery from hillslopes to control fluvial transport has not been tested. In
29 this contribution, we present a model linking the production of sediment through weathering
30 with a sediment transport model to explore the conditions leading to the formation of the Rio
31 Pisco terraces.

32

1 3 Hillslope Regolith

2 The mechanisms and rates of weathered regolith production are commonly expressed in the
3 context of erosion rates such that slower erosion rates are associated with thicker soil cover
4 (e.g. *Heimsath et al.*, 1997). The Western Andean margin of Peru provides a setting in which
5 weathered regolith is thick on the slowly eroding plateau, but nearly absent at low elevations
6 despite even lower erosion rates. This seeming contradiction is best explained by gradients in
7 the governing climatic variables. *White and Blum* (1995b) showed that solute fluxes from a
8 global compilation of granitic watersheds approach 0 as precipitation approaches 0. In order
9 to best model this gradient in soil thickness, we apply the climate dependent regolith
10 production model of *Norton et al* (2014), which was based on the temperature and
11 precipitation dependent weathering data of *White and Blum* (1995b). The model predicts
12 time-transgressive or steady state soil production rates and soil thicknesses for a given mean
13 annual temperature and mean annual precipitation, and mean erosion rate. Temperature (T),
14 precipitation (P), and silicate mineral activation energy (E_a) set the maximum soil production
15 rate (SPR_{\max}):

$$16 \quad SPR_{\max} = a_0 P e^{\frac{-E_a}{R} \left(\frac{1}{T} - \frac{1}{T_0} \right)}, \quad (1)$$

17 where R is the gas constant, T_0 is 5°C , and $a_0 = 0.42$ is a precipitation scaling factor tuned to
18 the Pisco soil dataset (*Norton et al.*, 2014). The instantaneous soil production rate (SPR) and
19 change in soil thickness are calculated as a function of soil depth (H);

$$20 \quad SPR = SPR_{\max} e^{-\alpha H}, \quad (2)$$

21 and local mass balance;

$$22 \quad \frac{dH}{dt} = a_0 P e^{\frac{-E_a}{R} \left(\frac{1}{T} - \frac{1}{T_0} \right)} e^{-\alpha H} - D, \quad (3)$$

23 where $\alpha = 0.03 \text{ cm}^{-1}$ is the soil depth scalar (e.g. *Heimsath et al.*, 1997) determined as the best
24 fit to the Pisco dataset (*Norton et al.*, 2014) and D is the denudation rate. Globally, α has been
25 measured between 0.017 and 0.042 cm^{-1} (*Heimsath et al.*, 2001; 2005). The highest values
26 result in slightly thinner soils that are equivalent within error to the modelled soil thicknesses
27 using $\alpha = 0.03 \text{ cm}^{-1}$ (see *Norton et al.*, 2014). Lower values of α result in significantly thicker
28 soils which would enhance river sediment loads during rapid soil stripping. Rapid soil

1 production rates and thick soils are predicted for high temperatures and precipitation amounts.
2 Erosion rates are the ultimate control on the output soil thickness and system response time.

3 **3.1 Regolith thickness in the Rio Pisco drainage basin**

4 We test the sensitivity of the *Norton et al.* (2014) model to the different input variables by
5 allowing one variable to change while holding the other two at the plateau value (Figure 5). In
6 the model, temperature and precipitation influence the maximum soil production rate
7 (Equation 1), while erosion determines the overall mass balance (Equation 3). Precipitation
8 and erosion have the largest individual control on the calculated steady-state regolith
9 thickness. The temperature effect is much smaller. As such, variations in temperature (both
10 intra- and inter-annual) are negligible compared to other parameters. If regolith thicknesses
11 were dependent on temperature alone, the model predicts a more or less uniform blanket over
12 the entire catchment, increasing slightly towards the coast as temperatures get warmer. In
13 contrast, regolith depth would decrease rapidly towards the coast in a solely precipitation-
14 dependent state, approaching 0 at ~100 km from the headwaters. Finally, if erosion were the
15 sole process controlling and limiting regolith thicknesses, the value of this variable would be
16 expected to decrease in the rapidly eroding knickzone, but to thicken again farther
17 downstream. We note that in all cases, a positive dependence of the maximum soil production
18 rate SPR_{max} on erosion, as proposed by *Heimsath et al.* (2012), would result in thicker soil
19 cover over a wider range of erosion rates, but should not change the overall distribution of
20 soils from the model. The modeled regolith depths generally match the sparse measured
21 depths from ridgetops in the Pisco Valley (e.g. *Norton et al.*, 2014). Ridgetops were sampled
22 for soil depth as the hillslopes throughout the escarpment tend to be stripped bare of
23 weathered material in the modern climate. Additionally, the rugged terrain, poor access and
24 lack of drillings precluded the collection of further data.

25

26 **3.2 Hillslope sediment delivery mechanisms**

27 Sediment supply to the river was calculated by combining the climate dependent soil
28 production model (*Norton et al.*, 2014) with cosmogenic nuclide-derived denudation rates
29 (*Abbühl et al.*, 2010, 2011; *Bekaddour et al.*, 2014). To determine modern sediment supply,
30 we allow the Pisco river to erode at its long-term rate as determined by cosmogenic nuclides,

1 assuming no hillslope storage (an assumption vital to the cosmogenic nuclide methods as
2 well; e.g. *von Blanckenburg, 2006*). The modern discharge is taken as the basin integrated
3 precipitation rate (*Agteca, 2010*), which decreases down river which yields an average
4 discharge of $20 \text{ m}^3 \text{ s}^{-1}$ along the coastal section. As such, we ignore the effects of
5 evapotranspiration and infiltration, but still capture a more realistic discharge for the Pisco,
6 which is c. $23 \text{ m}^3 \text{ s}^{-1}$ as measuring at the gauging station of Letrayoc (*Bekaddour et al., 2014*).

7 We model two potential responses to increased rainfall during pluvial periods: steady state
8 increase in denudation rate, and transient stripping of hillslope sediment (Figure 6). We
9 consider steady state to be the case where the soil production response time is significantly
10 shorter than the timescale over which long-term climate changes (i.e. soil transitions smoothly
11 between steady state thicknesses). Based on cosmogenic nuclide concentrations from the
12 Piura River in northwestern Peru, *Abbühl et al. (2010)* showed that, at steady state,
13 denudation rates increase exponentially with increasing precipitation rates below the plateau
14 edge but are independent of precipitation on the plateau. Our first model assumes this
15 relationship to hold in time as well as space. We therefore hold the denudation rate constant
16 on the plateau throughout time, but vary the denudation rate below the plateau edge as
17 $D_2 = D_1 * \exp^{cP}$ (where D_2 and D_1 are the predicted and initial denudation rate (mm yr^{-1}),
18 respectively, P is the mean annual precipitation (mm) and $c = 0.0041$ is empirically derived
19 for the Western Andes; *Abbühl et al., 2010*) up to the limit of soil thickness (i.e. the maximum
20 allowable erosion rate is the soil production rate).

21 The transient model is based on the widespread presence of debris flow deposits in the
22 terraces and the rapid accumulation rates suggested by OSL dating (*Steffen et al., 2009*).
23 These observations suggest that sediment is rapidly eroded from the hillslopes during pluvial
24 periods, resulting in a sediment pulse into the basin. To model this transient sediment
25 delivery, we assume complete hillslope stripping downstream of the knickzone (where slopes
26 are steep) upon initiation of the pluvial period followed by negligible erosion after the
27 hillslopes become bare of sediment (e.g. Figure 6). We compare the longitudinal sediment
28 transport capacity/sediment load ratios to the existing terrace distribution in the Pisco valley.

29

1 4 Fluvial transport

2 The eroded material delivered to the channels will either be deposited or transported,
3 depending on the transport capacity of the stream. Channel flow and potential incision in
4 these streams are typically expressed in terms of shear stress and sediment transport
5 equations, and flow is driven by temporally variable (but spatially homogeneous)
6 precipitation.

7 We begin by coupling the weathering-dependent model with an algorithm that describes
8 sediment transport in channels and apply it to the long profile of the Rio Pisco. Sediment
9 transport capacity T_c is calculated using the Bagnold equation (e.g. *Tucker and Slingerland*,
10 1994; 1997):

11

$$12 \quad T_c = \frac{BW}{(\rho_s - \rho_w)\rho^{1/2}g} (\tau - \tau_c)(\tau^{1/2} - \tau_c^{1/2}) \quad (4)$$

13

14 where B is a constant equal to 10 (e.g. *Hancock and Anderson*, 2002), W is channel width, ρ_s
15 and ρ_w are the densities of sediment and water, respectively, g is gravity, τ is the applied bed
16 shear stress, and τ_c is the critical shear stress for the entrainment of the D_{50} , which is the 50th
17 percentile grain size. Note that here we calculate sediment transport capacity, and the actual
18 sediment discharge is dependent on the sediment yield of the basin. We scale channel width to
19 catchment area A using the empirical geometry relationship, $W = aA^b$ (e.g. *Yalin*, 1992) fit to
20 the Rio Pisco, where a is 0.015 and b is 0.95 (Figure 7).

21 Shear stress is calculated as:

22

$$23 \quad \tau = \rho_w g \left(\frac{Q_w}{W} \right)^{3/5} n^{3/5} S^{7/10} \quad (5)$$

24

25 (after *Hancock and Anderson*, 2002) where Q_w is the water discharge, n is Manning's n , and S
26 is the channel gradient. Critical shear stress is calculated as

27

$$1 \quad \tau_c = 0.047(\rho_s - \rho_w)gD_{50} \quad (6)$$

2

3 (e.g. Leopold et al., 1964) where D_{50} is the 50th percentile grain size, here taken to be the
 4 mean grain size measured in the Pisco Valley terraces, 0.02 m (*Litty et al.*, 2015). We applied
 5 a Shield's parameter of 0.047, which is consistent with the suggestions proposed by *Meyer-*
 6 *Müller* (1948) and *Heller and Paola* (1992) for these streams.

7 The cumulative sediment supply is calculated as the sum of the upstream hillslope erosional
 8 fluxes contributing to point n along the channel:

9

$$10 \quad Q_s = \sum_{i=1}^n D_i A_i \quad (7)$$

11 and water discharge is likewise calculated as the sum of the upstream area and precipitation
 12 amount,

13

$$14 \quad Q_w = \sum_{i=1}^n c P_i A_i \quad (8)$$

15

16 where A_i is the lateral contributing hillslope area (m^2) to point i in the channel, P_i is
 17 precipitation (mm a^{-1}) and D_i is erosion (mm a^{-1}) from this area, and c is a runoff coefficient.
 18 The runoff coefficient accounts for losses due to evapotranspiration and infiltration. Because
 19 of a lack of data we assume in this study that $c=1$, however, it is likely that the coefficient is
 20 smaller as evapotranspiration (e.g., *Bloschl et al.*, 2013) and infiltration in the lower reaches
 21 of the Rio Pisco lead to lower discharge downstream. In this case, T_c will decrease more
 22 rapidly downstream.

23 The fluvial transport model, while simple in its approach, provides a first order estimate of
 24 river response in this system. The 1-D model is not capable of representing changes in fluvial
 25 transport style or changing hydraulic parameters. This is especially noticeable in our
 26 treatment of hydraulic geometry and shear stress which are calculated using empirical
 27 relationships (e.g. *Hancock and Anderson*, 2002; *Shields*, 1936). We adopted this approach as

1 a more formal treatment of roughness and skin friction (e.g. *Ferguson, 2007*) would require
2 knowledge of flow velocity or depth which are lacking for the Rio Pisco. Despite these
3 limitations, the shear stress approach has been shown to adequately model strath terrace
4 formation which involves both erosion and deposition in the fluvial system (*Hancock and*
5 *Anderson, 2002*).

6 **4.1 Coupled hillslope-river model**

7 We apply the 1-D coupled sediment transport - weathering dependent soil model to the Rio
8 Pisco using 1 km node spacing (Figure 6e, f). All dependent variables are free to change at
9 each node (e.g. spatially variable denudation rates, precipitation rate, and temperature). We
10 take precipitation rates from the Global Historical Climatology Network compilation of
11 *Agteca* (2010), which are based on 493 individual rain gauges measured over 10 to 85 years
12 (mean 20 years) within Peru. For the Rio Pisco model inputs (Figure 2), we use the long-
13 profile trend of precipitation based on an interpolation of the 17 rain gauges that are within 25
14 km of the catchment. The largest inter-annual variability occurs on the plateau where annual
15 rainfall is the highest. Relative rates are, however, highest near the coast where large single
16 events can more than double the annual averages (Figure 8b). *Garraud et al. (2003)* used an
17 atmospheric transport which excluded ocean dynamics model to estimate glacial-interglacial
18 climate on the Altiplano. Their ~10-20% modelled glacial-interglacial precipitation variability
19 through the Late Quaternary matches the ~16-18% inter-annual variability on the Altiplano
20 from the *Agteca* (2010) dataset. As such, we assume that the 20 year data are at least broadly
21 representative of long-term precipitation and use the relationship between absolute
22 precipitation rate and relative variability (Figure 8b) to test the sensitivity of the model and
23 propagate errors. Both sediment transport capacity and sediment load are dependent on
24 precipitation. Decreased precipitation on the plateau could lead to transport limited streams
25 through decreased sediment transport capacity (Figure 9). Otherwise, within realistic limits,
26 precipitation does not significantly change our results.

27 Temperature is determined for each node assuming an atmospheric lapse rate of $6^{\circ}\text{C km}^{-1}$,
28 and the mean annual temperature of 12.8°C of Cusco, Peru at 3204m elevation a.s.l.
29 Temperatures during the Last Glacial Maximum are estimated to have been $5\text{-}9^{\circ}\text{C}$ lower on
30 the Altiplano (*Baker et al., 2001*). The sensitivity of the coupled model to temperature is
31 tested within the glacial/interglacial variability. As temperature only affects the maximum soil

1 production rate it has no effect on the transport capacity or the sediment load on the plateau
2 where erosion rates are held constant (Figure 9).

3

4 Denudation rates for the Rio Pisco have been measured by *Abbühl et al.* (2010) and
5 complemented by *Bekaddour et al.* (2014). We use a tensioned spline (weight 0.1) to
6 interpolate denudation rate values for each point along the river profile. Denudation rates
7 reach a maximum of $\sim 250 \text{ mm a}^{-1}$ in the knickzone and are much lower on both the plateau
8 and near the coast at $\sim 11 \text{ mm a}^{-1}$. We exclude one sample (Pis 11) from the dataset of *Abbühl*
9 *et al.* (2011) as it is most likely heavily influenced by recycling of shielded sand from the ~ 50
10 ka conglomerate terraces and therefore does not represent the basin-wide denudation rate at
11 this point. These long-profile values are used as inputs to calculate soil depths along the Pisco
12 Valley and to determine sediment delivery to the channel. Sediment load is controlled by
13 erosion rate in the model. At very rapid erosion rates, the sediment loads may exceed
14 transport capacity on the plateau (Figure 9). In all other scenarios, erosion variation does not
15 change our results.

16

17 **4.2 Sediment load and transport**

18 Calculated modern sediment transport capacity and sediment flux (determined from ^{10}Be
19 derived denudation rates (*Abbühl et al.*, 2010) show that the transition from supply limit to
20 transport limit coincides with the upstream appearance of terraces (Figure 10). Note that
21 supply and transport limits refer in this case to excess transport capacity and sediment load,
22 respectively. We also acknowledge that the terrace sediments represent primarily the bedload
23 flux while the cosmogenic nuclide-derived sediment flux is total load (i.e. dissolved,
24 suspended, and bedload). This is because cosmogenic nuclides record total land surface
25 lowering, whether through chemical or physical weathering and terraces are by necessity built
26 only of the physical load. As such, our estimated sediment loads are likely a maximum. Even
27 with this caveat, the stream is supply limited in the upper bedrock-floored sections, and
28 transport limited further down where cut-fill terraces are abundant, and the modern river
29 flows over a wide floodplain made up of gravelly sediments. In the case that the Rio Pisco
30 basin maintains steady-state (e.g. the response time of the weathering system is faster than the
31 rate of climate change), the main response to a doubling of precipitation rates (using eq. 8 for

1 water flux, and eq. 7 for the erosional flux) from modern is for the stream to aggrade over a
2 relatively short ~20 km long section below the knickzone (Figure 10b). During drier climates,
3 the sediment transport capacity in this zone exceeds the loads as denudation rates are low.
4 According to this simulation of wet and dry steady-states, extensive cut-and-fill terraces
5 should only be common in a narrow band near the knickzone. Farther downstream, sediment
6 flux exceeds sediment transport capacity both during wet and dry phases and the stream
7 primarily aggrades.

8 A transient stripping scenario is suggested by the results of *Steffen et al.* (2009). According to
9 Figure 3 in their paper, the transition towards a more humid climate resulted in an episodic
10 phase of erosion, where regolith was rapidly stripped from hillslopes below the plateau over
11 ~10-15 ka, supplying large volumes of sediment to the trunk stream. These phases of fluvial
12 aggradation are followed by waves of incision travelling back up valley. This suggests that an
13 episodic phase of rapid hillslope stripping occurs, resulting in a large sediment pulse to the
14 rivers, followed by a rapid drop off of hillslope-derived sediment as the hillslope reservoirs
15 are emptied. We model this transient response towards a more humid climate as a two-step
16 process. Upon initiation of the wet period, all weathered regolith (calculated from the model)
17 below the plateau is stripped from the hillslopes and supplied to the stream. In the second
18 step, the bare hillslopes are unable to contribute new sediment to the stream. This is
19 exacerbated by potentially faster erosion rates during the wet phases that inhibit the formation
20 of a significant regolith cover. In this scenario, sediment supply to the stream during this step
21 is controlled solely by inputs from the plateau, with little to no sediment being supplied from
22 below the plateau. This pulsed-transient case necessitates that sufficient time has elapsed
23 between wet periods for the weathered regolith to build up to the steady state values
24 (*Bekaddour et al.*, 2014). This is the case for the ~10 ka climate intervals in western Peru. For
25 the Rio Pisco knickzone, modern erosion rates range from ~50-250 mm a⁻¹ (*Abbühl et al.*,
26 2011) with annual precipitation between ~100 and 400 mm (*Agteca*, 2010). This results in soil
27 response times (90% of the steady state value) of 5.3 – 25 ka (*Norton et al.*, 2014). The result
28 of this simulation is that sediment accumulates over the entire downstream reach of the stream
29 as regolith is rapidly stripped from the hillslopes. Once this material is exhausted, however,
30 the bedrock-alluvial transition moves approximately 100 km upstream, incising the valley fill
31 (Figure 10c). This scenario is more consistent with the observed occurrence of terraces in the
32 Rio Pisco (Figure 3). This scenario is also supported by ¹⁰Be-derived paleodenudation rates
33 (Figure 11; *Bekaddour et al.*, 2014). The first sediments deposited during each wet phase are

1 debris flow breccias with high ^{10}Be concentrations (lower palaeodenudation rates), indicative
2 of long residence time on the hillslopes. The subsequent fluvial gravels are derived from
3 sediment with shorter residence times (higher palaeodenudation rates). The continued
4 contribution of fluvial sediment with high palaeodenudation rates suggests that reality most
5 likely lies between the steady-state and pulsed-transient cases. However, these end-member
6 scenarios can be informative for understanding terrace formation in escarpment environments
7
8

9 **5 Discussion and Conclusion**

10 Fluvial aggradation in the Rio Pisco has been associated with wet periods (*Steffan et al.*,
11 2009). This has important consequences for regolith production on the Western Escarpment.
12 On the plateau, where precipitation rates are $\sim 1000 \text{ mm a}^{-1}$ and denudation rates $\sim 10 \text{ mm a}^{-1}$,
13 the response time of soils is $> 100 \text{ ka}$ (*Norton et al.*, 2014). In the knickzone, precipitation is
14 $\sim 100\text{-}400 \text{ mm a}^{-1}$ and denudation rates are $100\text{-}250 \text{ mm a}^{-1}$. This results in soil response times
15 of $\sim < 10 \text{ ka}$. More importantly, the knickzone reach lies in a special climatic and denudational
16 setting in which small decreases in precipitation or increases in denudation can push the
17 system into a state where regolith production rates are unable to keep up with denudation.
18 Once conditions become amenable to regolith formation again, cover can reform on
19 millennial timescales on the hillslopes due to the rapid response times (*Norton et al.*, 2014).

20 When applied to the modern Rio Pisco the model suggests transient behavior. On the long
21 term, knickzone migration is eroding into the plateau as the river adjusts to a lower baselevel.
22 In addition to the direct control that baselevel has on the river, undercutting can dramatically
23 change the rates and style of hillslope response (*Roering et al.*, 2015; *Bilderbach et al.*, 2015).
24 In the Pisco Valley case, little sediment is available in the knickzones and response may
25 resemble the Waipaoa catchment in New Zealand where baselevel lowering generated
26 abundant deep-seated landslides (*Bilderbach et al.*, 2015). Such a response is partially
27 supported by the presence of large boulders in the channels and coarse-angular clasts in the
28 debris flow deposits. On the short term, hillslopes are quickly stripped of sediment,
29 decoupling hillslope regolith from the incising channel. Key to both of these processes is that
30 the timescale of hillslope stripping (as implied by the occurrence of debris flows) is less than
31 the timescale of regolith production. For instance, an increase in precipitation rates can lead to
32 a temporary increase in denudation rates (*Tucker and Slingerland*, 1997) until the hillslopes

1 are stripped of sediment, exposing bedrock (*Carson and Kirkby, 1972*). The regolith is then
2 regenerated during intermediate climates. An additional complication, recently suggested by
3 *Heimsath et al.* [2012], is that the maximum regolith production rate may also be dependent
4 on erosion rates such that faster erosion rates yield faster production rates. While we have not
5 built this relationship into this study; we note that such a relationship would lead to enhanced
6 regolith thickness in the knickzones and have no effect on the slowly eroding plateau or
7 coastal plains.

8 The model clearly shows that regolith production on hillslopes has a large impact on
9 sediment-flux in the river. The sequences of cut-fill terraces observed in the Rio Pisco are
10 more consistent with transient hillslope stripping during wet phases, followed by incision
11 once the hillslopes are bare of regolith. This can have significant consequences for the
12 evolution of bedrock streams in particular, where incision rates are at least partially dependent
13 on sediment flux (*Whipple and Tucker, 2002*). It is interesting to note that much the terraced
14 zone does not adhere to the definition of a bedrock channel presented by *Turowski et al.*
15 (2008) since much of the erosion is acting on previous fill. In this case, the bedrock/alluvial
16 transition of *Tucker and Slingerland* (1996) is better defined as underload/overload with the
17 result being local erosion or deposition of the substrate, be it bedrock or sediment. Large
18 changes in sediment delivery will also result in significant changes in hydraulic geometry,
19 channel gradient, and erosion regime both at-a-station and downstream. Deposition during
20 high sediment load phases would flatten and widen the rivers, temporarily reducing driving
21 stress. For the transient case presented here, this would enhance the modelled relationship
22 leading to larger variation between erosional and depositional phases.

23 The occurrence of cut-fill terraces in the Rio Pisco is best explained by a pulsed-transient
24 response in which increased precipitation rates strip hillslopes of weathered material. The
25 hillslopes remain bare until climate again becomes amenable to the preservation of weathered
26 regolith. Such a scenario could be important in other escarpment settings.

27

28 **Acknowledgements**

29 The authors would like to thank M. Trauerstein and T. Bekaddour for assistance in the field.
30 Two anonymous reviews and excellent editorial handling by Simon Mudd have improved the

1 manuscript. This work was supported in part by a VUW Faculty of Science grant to KPN and
2 SNF grant 200020_155892 awarded to FS.
3

1 **References**

- 2 Abbühl, L.M., Norton, K.P., Jansen, J., Schlunegger, F., Aldahan, A., and Possnert, G.:
3 Landscape transience and mechanisms of knickpoint retreat from ^{10}Be in the Western
4 Escarpment of the Andes between Peru and northern Chile, *Earth Surface Processes and*
5 *Landforms*, 36, 1464-1473, 2011.
- 6 Abbühl, L. M., Norton, K. P., Schlunegger, F., Kracht, O., Aldahan, A., and Possnert, G.: En
7 Niño forcing on ^{10}Be -based surface denudation rates in the northwestern Peruvian Andes?,
8 *Geomorphology*, 123, 257-268, 2010.
- 9 Agteca: Global Historical Climatology Network (GHCN-Monthly database) compilation for
10 Peru, edited, Cochrane, T.A., Agteca.org, 2010.
- 11 Baker, P.A., Rigsby, C.A., Seltzer, G.O., Fritz, S.C., Lowenstein, T.K., Bacher, N.P., and
12 Veliz, C.: Tropical climate changes at millennial and orbital timescales on the Bolivian
13 Altiplano, *Nature*, 409, 698-701, 2001a.
- 14 Baker, P.A., Seltzer, G.O., Fritz, S.C., Dunbar, R.B., Grove, M.J., Tapia, P.M., Cross, S.L.,
15 Rowe, H.D., and Broda, J.P.: The History of South American Tropical Precipitation for the
16 Past 25,000 Years, *Science*, 291, 640-643, 2001b.
- 17 Bekaddour, T., Schlunegger, F., Vogel, H., Delunel, R., Norton, K.P., Akcar, N., and Kubik,
18 P.K.: Paleo erosion rates and climate shifts recorded by Quaternary cut-and-fill sequences in
19 the Pisco valley, central Peru, *Earth and Planetary Science Letters*, 390, 103-115, 2014.
- 20 Bilderback, E. L., Pettinga, J. R., Litchfield, N. J., Quigley, M., Marden, M., Roering, J. J.,
21 and Palmer, A.S.: Hillslope response to climate-modulated river incision in the Waipaoa
22 catchment, East Coast North Island, New Zealand, *Geological Society of America Bulletin*,
23 127, 131-148, 2015.
- 24 Blöschl, G., Sivapalan, M., Wagener, T., Viglione, A., and Savenije, H.: *Runoff Prediction in*
25 *Ungauged Basins. Synthesis across Processes, Places and Scales* Cambridge University press,
26 2013.
- 27 Bookhagen, B., and Strecker, M.R.: Orographic barriers, high-resolution TRMM rainfall, and
28 relief variations along the eastern Andes, *Geophysical Research Letters*, 35, 2008.

1 Bookhagen, B., D. Fleitmann, K. Nishiizumi, M. R. Strecker, and Thiede, R.C.: Holocene
2 monsoonal dynamics and fluvial terrace formation in the northwest Himalaya, India, *Geology*,
3 34, 601-604, 2006.

4 Carson, M. A., and Kirkby, M.J.: *Hillslope Form and Process*, Cambridge University Press,
5 Cambridge, 1972.

6 Fritz, S.C., Baker, P.A., Lowenstein, T.K., Seltzer, and Rigsby, C.A.: Hydrologic variation
7 during the last 170,000 years in the southern hemisphere tropics of South America,
8 *Quaternary Research*, 61, 95-104, 2004.

9 Garreaud, R., Vuille, M., Clement, A.C.: The climate of the Altiplano: observed current
10 conditions and mechanisms of past changes. *Palaeogeography, Palaeoclimatology,*
11 *Palaeoecology*, 194, 5–22, 2003.

12 Hancock, G.S., and Anderson, R.S.: Numerical modeling of fluvial strath-terrace formation in
13 response to oscillating climate, *Geological Society of America Bulletin*, 114, 1131-1142,
14 2002.

15 Heller P.L., and Paola, C.: The large-scale dynamics of grain-size variation in alluvial basins
16 2: application to syntectonic conglomerate: *Basin Research*, 4, 91– 102, 1992.

17 Heimsath, A.M., Dietrich, W.E., Nishiizumi, K., and Finkel, R.C.: The soil production
18 function and landscape equilibrium, *Nature*, 388, 358-361, 1997.

19 Heimsath, A.M., Chappell, J., Dietrich, W.E., Nishiizumi, K., Finkel, R.C.: Late Quaternary
20 erosion in southeastern Australia: a field example using cosmogenic nuclides. *Quaternary*
21 *International*, 83, 169–185, 2001.

22 Heimsath, A.M., Furbish, D.J., Dietrich, W.E.: The illusion of diffusion: field evidence for
23 depth-dependent sediment transport, *Geology*, 33, 949–952, 2005.

24 Heimsath, A.M., R.A. DiBiase, and Whipple, K.X.: Soil production limits and the transition
25 to bedrock-dominated landscapes, *Nature Geoscience*, 1-5, 2012.

26 Kober, F., F. Schlunegger, G. Zeilinger, and Schneider, H.: Surface uplift and climate change:
27 the geomorphic evolution of the Western Escarpment of the Andes of northern Chile between
28 the Miocene and present, *Geological Society of America, Special Paper 398*, 97-120, 2006.

29 Leopold, L.B., M.G. Wolman, and Miller, J.P.: *Fluvial processes in geomorphology*, W.H.
30 Freeman and Company, San Francisco, 1964.

1 Litty, C., Duller, R., and Schlunegger, F.: Paleohydraulic reconstruction of a 40 kyr-old
2 terrace sequence implies that water discharge was larger than today, *Earth Surface Processes*
3 *and Landforms*, in press.

4 Matmon, A., P. Bierman, and Enzel, Y.: Pattern and tempo of great escarpment erosion,
5 *Geology*, 30, 1135-1138, 2002.

6 McPhillips, D., Bierman, P.R., and Rood, D.H.: Millennial-scale record of landslides in the
7 Andes consistent with earthquake trigger, *Nature Geoscience*, 7, 925-930, 2014.

8 Meyer-Peter, E., and Müller, R.: Formulas for Bed-Load transport, *Proceedings of the 3rd*
9 *Conference, International Association of Hydraulic Research, Stockholm, Sweden* 39–64,
10 1948.

11 Norton, K.P., Molnar, P., and Schlunegger, F.: The role of climate-driven chemical
12 weathering on soil production, *Geomorphology*, 204, 510-517, 2014.

13 Placzek, C., Quade, J., and Patchett, P.J.: Geochronology and stratigraphy of late Pleistocene
14 lake cycles on the southern Bolivian Altiplano: Implications for causes of tropical climate
15 change, *Geological Society of America Bulletin*, 118, 515-532, 2006.

16 Roering, J. J., Mackey, B. H., Handwerger, A. L., Booth, A. M., Schmidt, D. A., Bennett, G.
17 L., and Cerovski-Darriau, C.: Beyond the angle of repose: A review and syn- thesis of
18 landslide processes in response to rapid uplift, Eel River, Northern California,
19 *Geomorphology*, 236, 109-131, 2015.

20 Schildgen, T. F., K. V. Hodges, K. X. Whipple, P. W. Reiners, and Pringle, M.S.: Uplift of
21 the western margin of the Andean plateau revealed from canyon incision history, southern
22 Peru, *Geology*, 35, 523-526, 2007.

23 Schlunegger, F., G. Zeilinger, A. Kounov, F. Kober, and Hüsser, B.: Scale of relief growth in
24 the forearc of the Andes of Northern Chile (Arica latitude, 18°S), *Terra Nova*, 18, 217-223,
25 2006.

26 Seidl, M. A., J. K. Weissel, and Pratson, L.F.: The kinematics and pattern of escarpment
27 retreat across the rifted continental margin of SE Australia, *Basin Research*, 8, 301-316, 1996.

28 Shields, A.: Anwendung der Ähnlichkeitsmechanik und der Turbulenzforschung auf die
29 Geschiebebewegung, *Mittlung der preussischen Versuchsanstalt für Wasserbau und*
30 *Schiffbau*, 26. (Berlin), 1936.

1 Steffen, D., F. Schlunegger, and Preusser, F.: Drainage basin response to climate change in
2 the Pisco valley, Peru, *Geology*, 37, 491-494, 2009.

3 Tucker, G. E., and Slingerland, R.L.: Erosional dynamics, flexural isostasy, and long-lived
4 escarpments: a numerical modeling study, *Journal of Geophysical Research-Solid Earth and*
5 *Planets*, 99, 12,229-12,243, 1994.

6 Tucker, G. E., and Slingerland, R.L.: Drainage basin responses to climate change, *Water*
7 *Resources Research*, 33, 2031-2047, 1997.

8 Turowski, J.M., Hovius, N., Wilson, A., and Horng, M-J.: Hydraulic geometry, river sediment
9 and the definition of bedrock channels, *Geomorphology*, 99, 26-38, 2008.

10 van der Beek, P., Summerfield, M. A., Braun, J., Brown, R. W., and Fleming, A.: Modeling
11 postbreakup landscape development and denudational history across the southeast African
12 (Drakensberg Escarpment) margin, *Journal of Geophysical Research-Solid Earth*, 107(B12),
13 2002.

14 Vanacker, V., von Blanckenburg, F., Hewawasam, T., and Kubik, P.W.: Constraining
15 landscape development of the Sri Lankan escarpment with cosmogenic nuclides in river
16 sediment, *Earth and Planetary Science Letters*, 253, 402-414, 2007.

17 von Blanckenburg, F.: The control mechanisms of erosion and weathering at basin scale from
18 cosmogenic nuclides in river sediment, *Earth And Planetary Science Letters*, 242, 223-239,
19 2006.

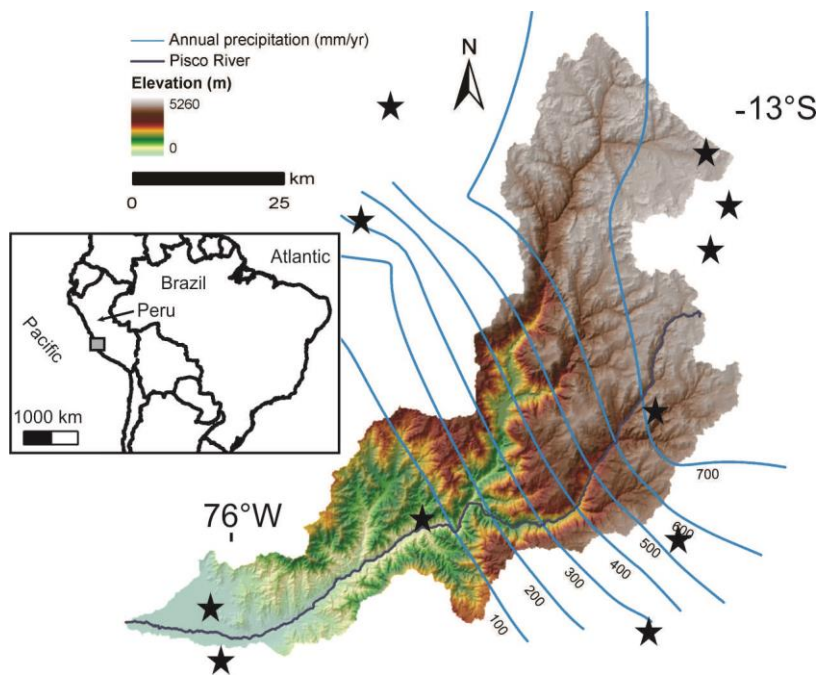
20 von Blanckenburg, F., Hewawasam, T., and Kubik, P.W.: Cosmogenic nuclide evidence for
21 low weathering and denudation in the wet, tropical highlands of Sri Lanka, *Journal of*
22 *Geophysical Research-Earth Surface*, 109(F3), 2004.

23 Weissel, J. K., and Seidl, M.A.: Influence of rock strength properties on escarpment retreat
24 across passive continental margins, *Geology*, 25, 631-634, 1997.

25 Whipple, K. X., and Tucker, G.E.: Implications of sediment-flux-dependent river incision
26 models for landscape evolution, *Journal of Geophysical Research*, 107, 1-20, 2002.

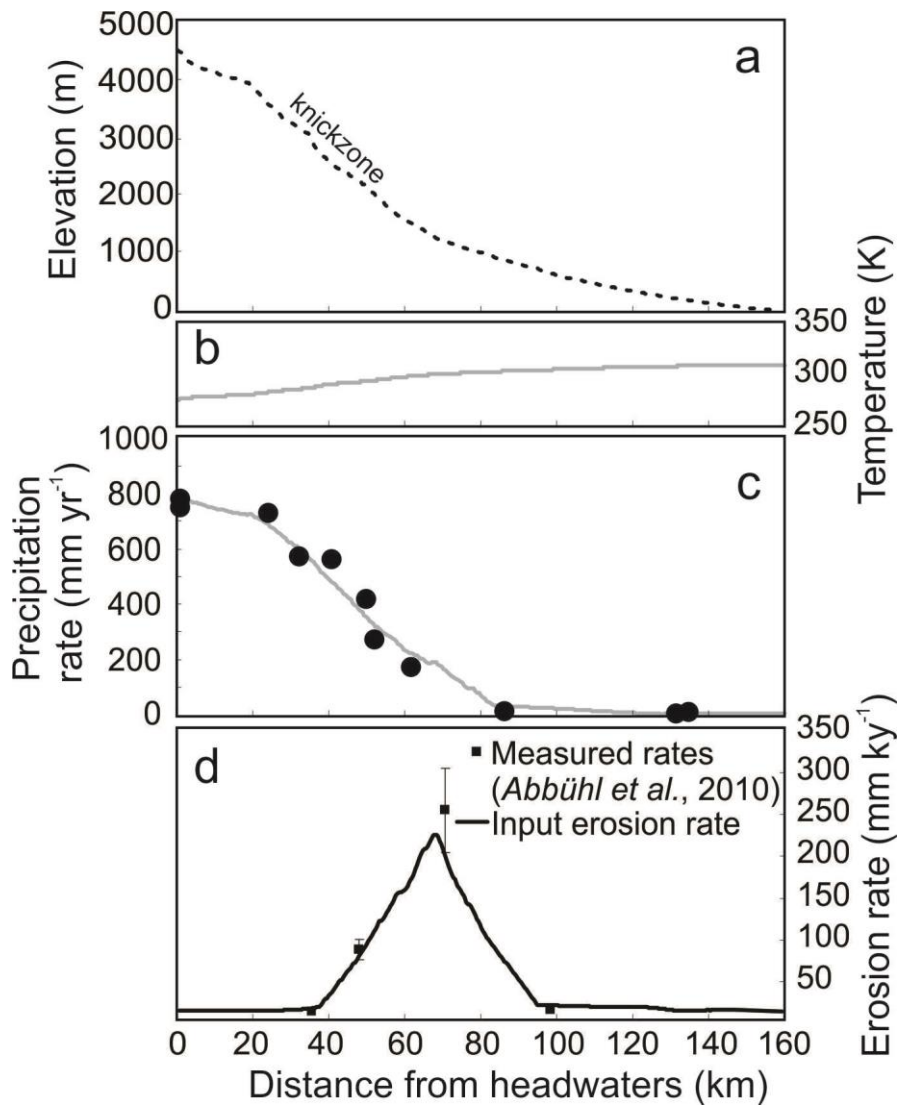
27 White, A. F., and Blum A.E.: Climatic effects on chemical weathering in watersheds;
28 application of mass balance approaches, in *Solute modelling in catchment systems*, edited by
29 S. T. Trudgill, 101-131, 1995a.

- 1 White, A. F., and Blum, A.E.: Effects of climate on chemical weathering in watersheds,
- 2 *Geochimica et Cosmochimica Acta*, 59, 1729-1747, 1995b.
- 3 Willet, S.D., McCoy, S.W., Perron, J.T., Goren, L., and Chen, C-Y.: Dynamic Reorganization
- 4 of River Basins, *Science* 343, 1249765-1-9.
- 5 Yalin, M. S.: *River Mechanics*, 219 pp., Pergamon, Tarrytown, N.Y., 1992.
- 6



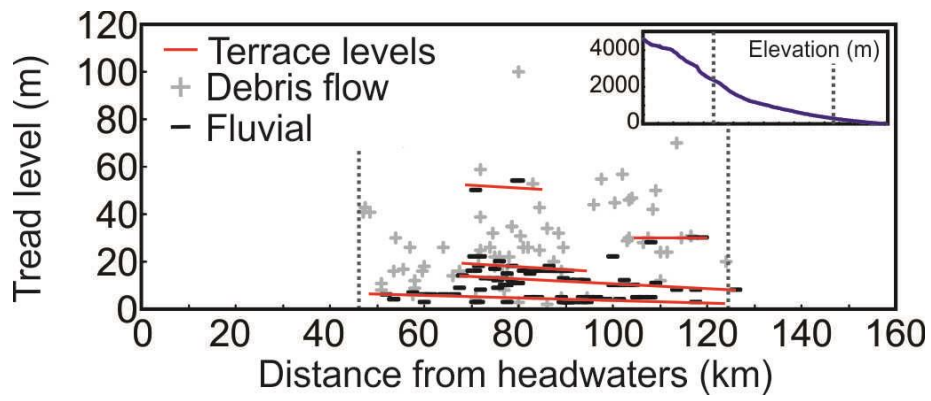
1
2
3
4
5

Figure 1. Setting and geomorphology of the Pisco River. Precipitation stations used to interpolate the annual rainfall are starred (Agteca, 2010).



1
2
3
4
5
6
7
8
9

Figure 2. Geomorphic and climatic input parameters along the the Pisco River including: (a) river longitudinal profile, (b) temperature, (c) annual precipitation, and (d) erosion rate. Input rainfall stations (*Agteca*, 2010) projected along strike onto the Pisco River profile are shown by closed dots, input erosion rates with errors (*Abbühl et al.*, 2011) are shown by closed squares. Downstream erosion rates were estimated by spatially interpolating the erosion rate data of *Abbühl et al.* (2011) and extracting the long-profile.

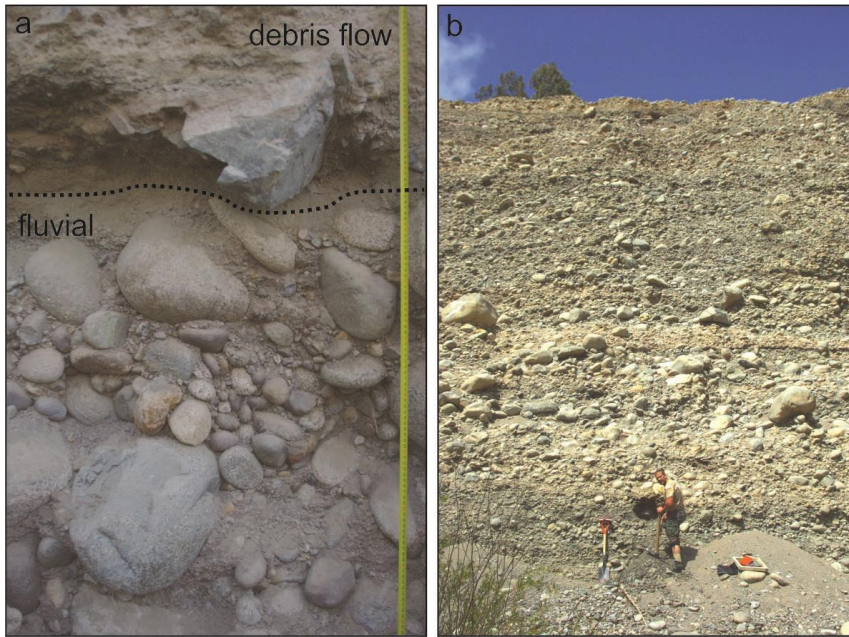


1

2

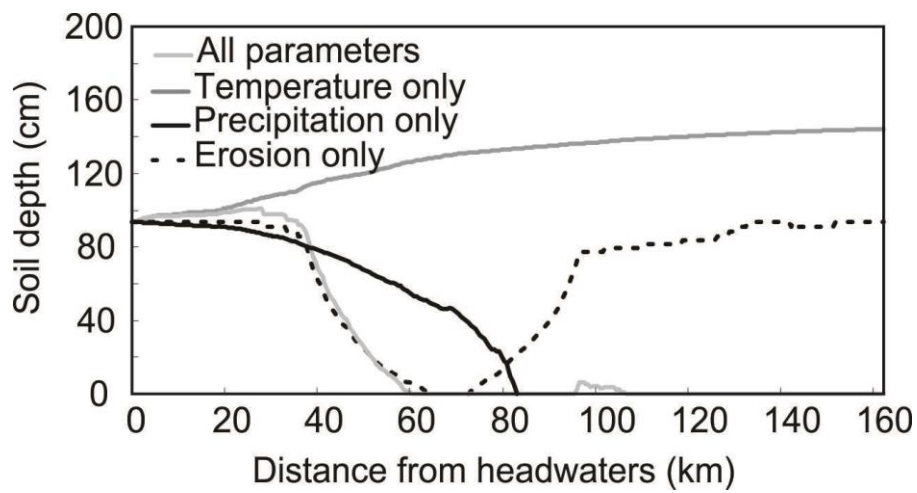
3 Figure 3. Locations of terraces along the Pisco River. The majority of terraces are
 4 concentrated in the zone from ~50 to 120 km downstream. Inset shows the location of the
 5 terraces (dashed lines) along the river profile.

6



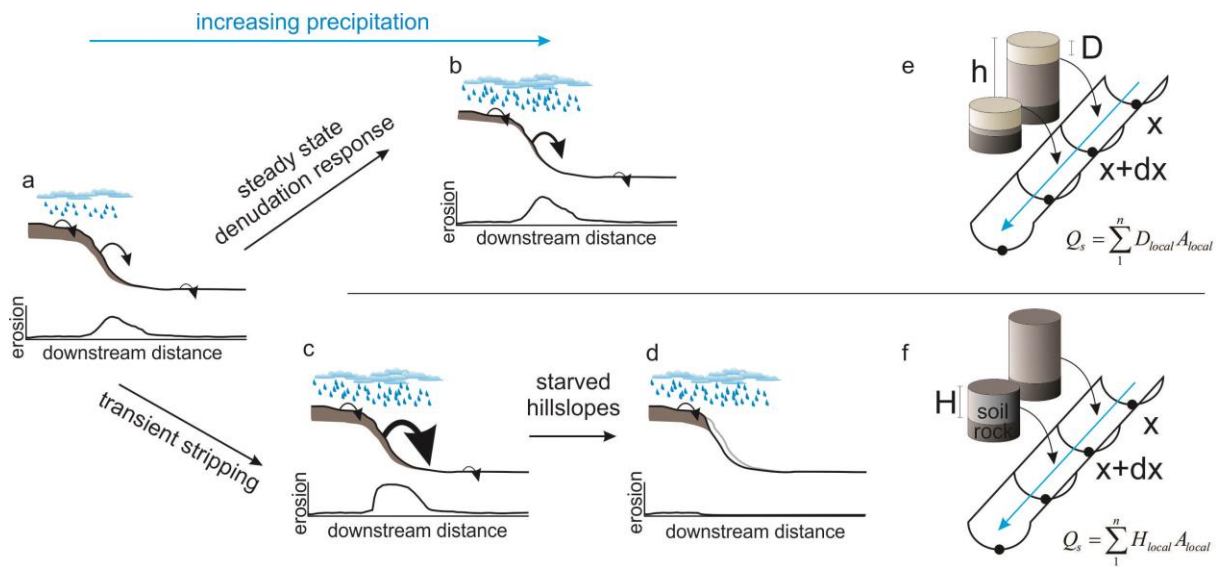
1
2
3
4
5
6

Figure 4. Rapid soil stripping in the Pisco valley is evidenced by abundant debris flow deposits (top, a) mixed with coarse, poorly sorted fluvial deposits (bottom, a and b, note person for scale).

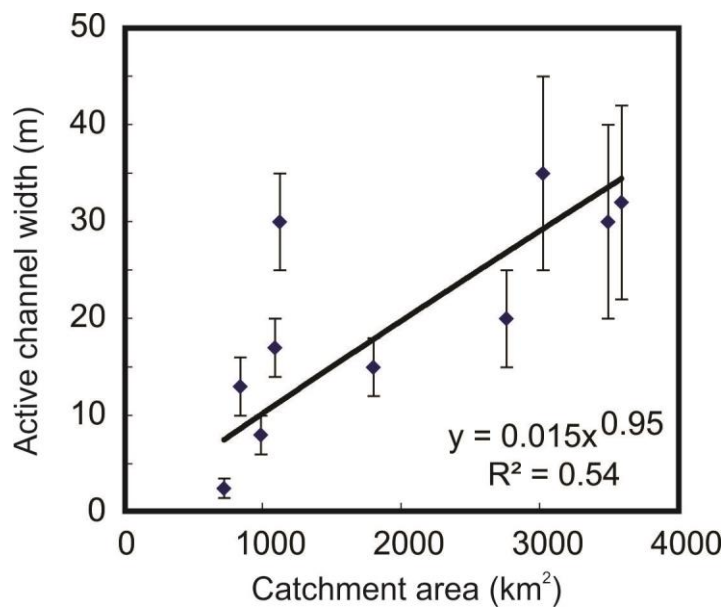


1
2
3
4
5
6
7
8

Figure 5. Sensitivity of the *Norton et al. (2014)* soil production model to each input parameter for the longitudinal profile of the Rio Pisco. The light grey line shows predicted soil thickness in the downstream direction using all parameters. We then held all other variables constant and allowed the temperature (medium grey line), precipitation (black line), and erosion (dashed line) to change downstream.

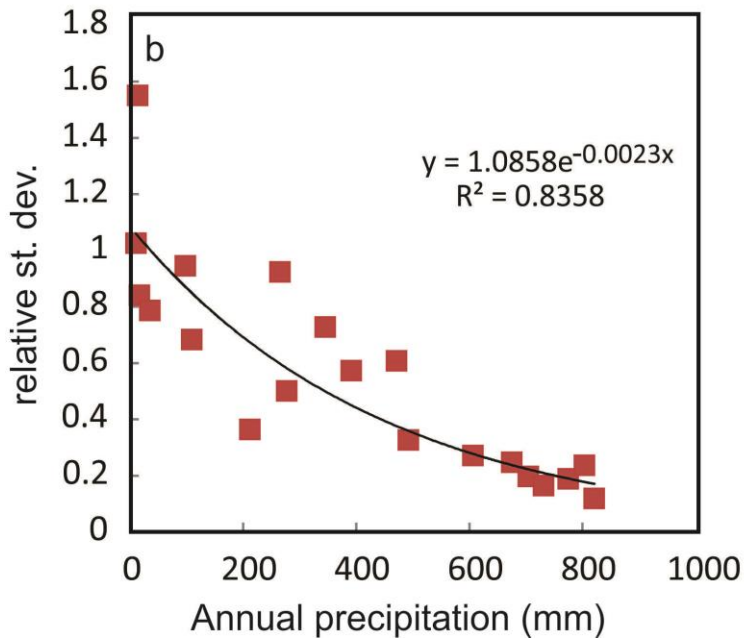
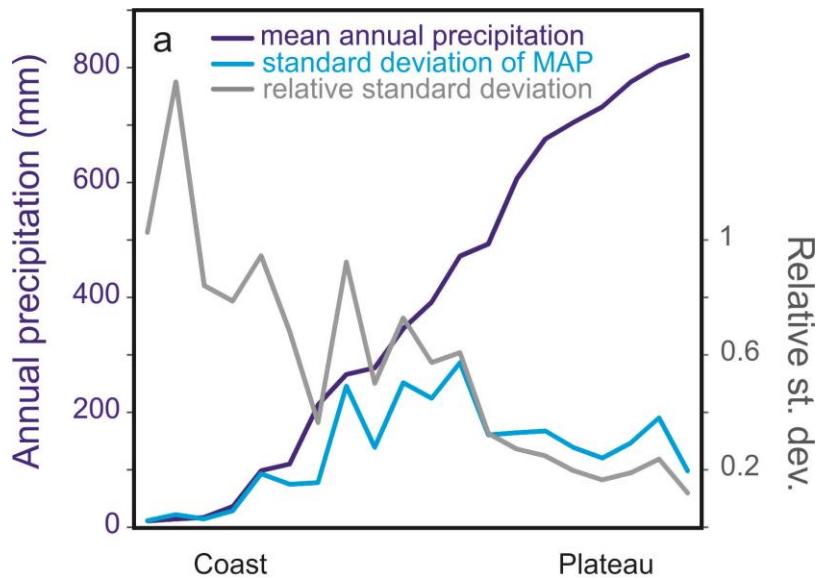


1
 2 Figure 6. Conceptual model of two modes of hillslope response to increased precipitation in
 3 semi-arid environments. Arrow size represents the relative contribution of eroded hillslope
 4 sediment to the river. In the steady state case (a-b), increased precipitation results in increased
 5 hillslope erosion rates on steep hillslopes which are balanced by increased soil production
 6 (e.g. Norton *et al.*, 2014). In the transient case (a-c-d), increased precipitation results in rapid
 7 stripping of hillslope sediment as debris flows and shallow landslides (c), followed by
 8 negligible erosion on steep hillslopes once the soil mantle is eroded (d). The model set up for
 9 each of these scenarios is shown in e (steady state) and f (transient stripping). The steady state
 10 model (e) calculates the sediment load Q_s as the sum of sediment delivered by erosion
 11 (erosion rate \times timestep \times local area) at each node. To model transient hillslope stripping, we
 12 remove the entire soil thickness (soil thickness \times timestep \times local area) at each node. These
 13 model setups provide endmember scenarios for hillslope response to changing climate.
 14



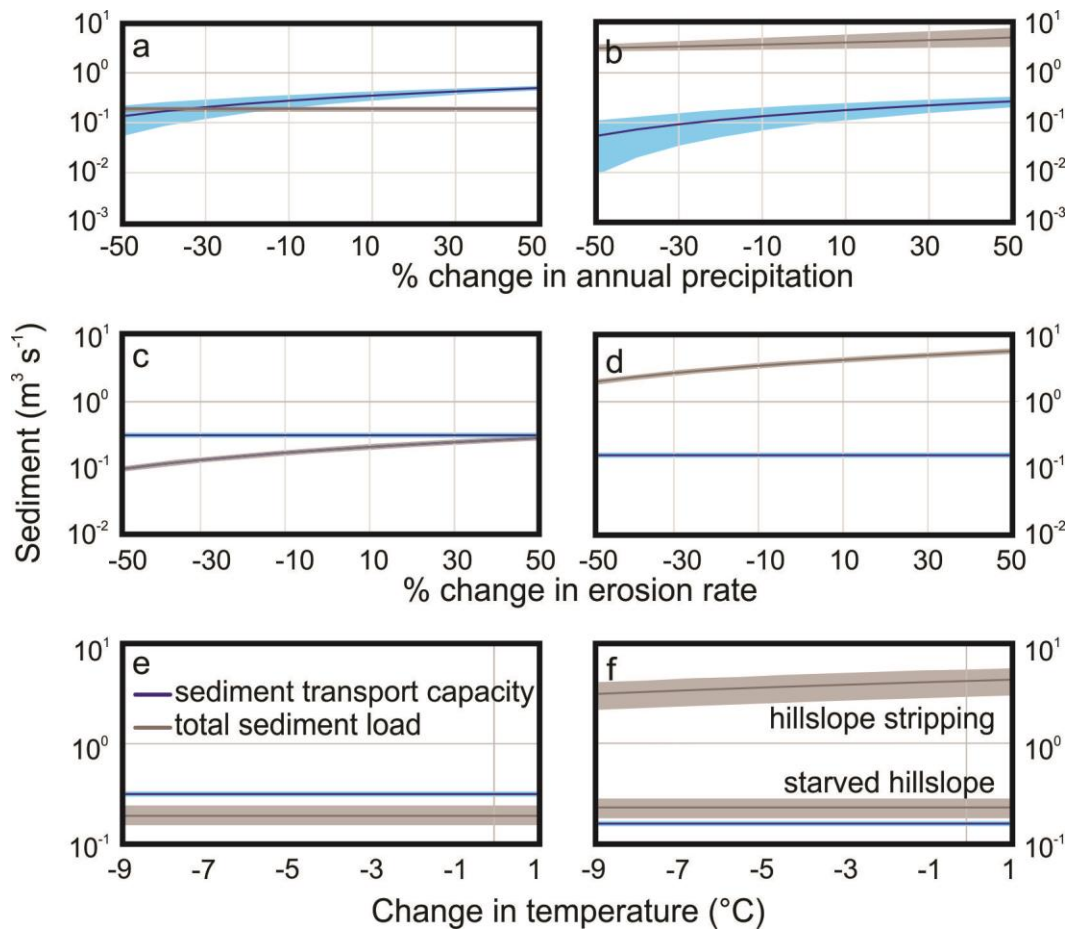
1

2 Figure 7. Active channel width/area scaling for the Rio Pisco.

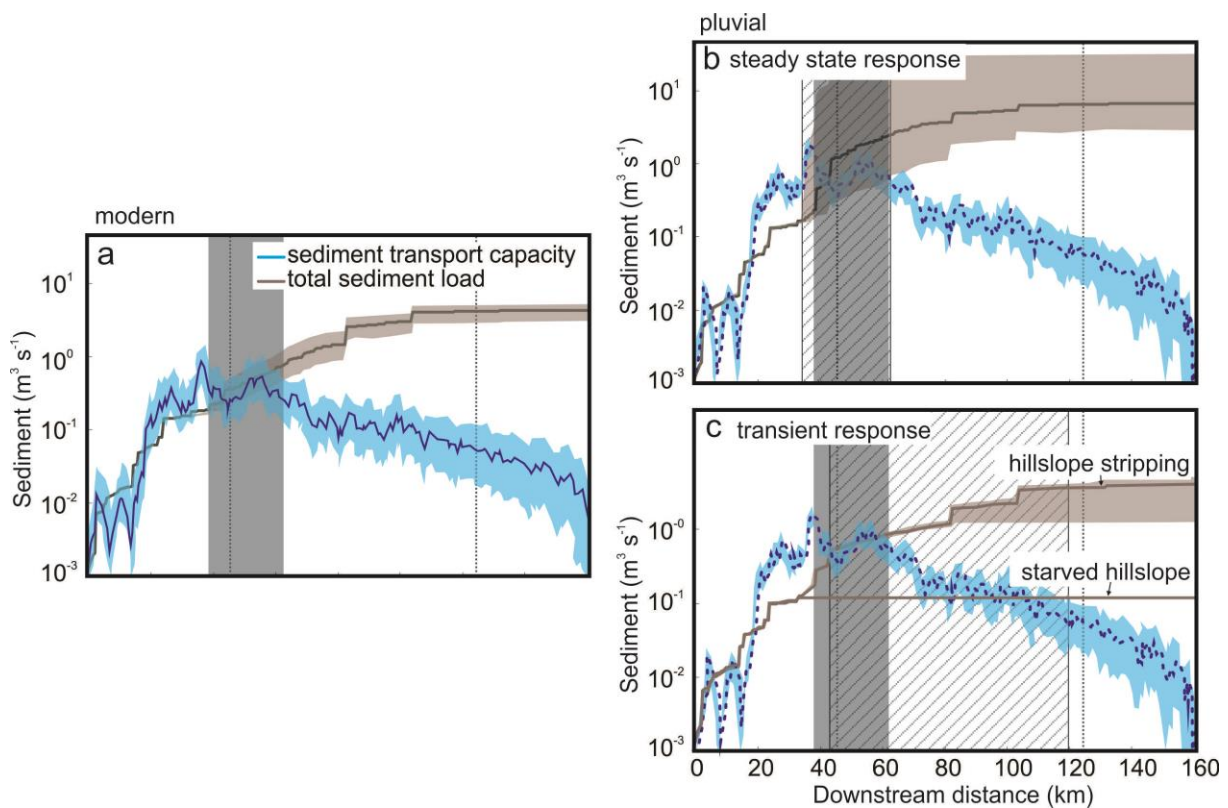


1

2 Figure 8. Variation in annual precipitation calculated from 20 year monthly averages
 3 (*Agteca*, 2010). The relative interannual variability is largest near the coast where El Nino
 4 years bring increased precipitation (a). The relationship between relative variability and
 5 annual precipitation (b) was applied to the soil production and transport models and carried
 6 through as uncertainty (Figures 9 and 10).



1
 2 Figure 9. Response of sediment transport capacity (blue lines) and total sediment load
 3 (brown lines) to changes in annual precipitation (a, b), erosion rate (c, d), and temperature
 4 (e, f) for nodes on the plateau 30km downstream (a, c, e) and beyond the knickzone 100
 5 km downstream (b, d, f). Each variable was changed within the estimated range for
 6 glacial/interglacial fluctuations (*Baker et al.*, 2001; *Garaud et al.*, 2003). The uncertainty
 7 for precipitation response (a, b) is propagated from the modern variability (*Agteca*, 2010;
 8 Figure 7). We assume an average 10% uncertainty in erosion rates (c, d) derived from
 9 cosmogenic nuclides and a 30% uncertainty in temperature (e, f) reflecting large
 10 uncertainties in the lapse rate. In all cases, the long-term variability does not likely change
 11 our model results. The exception to this is that sediment transport capacity on the plateau
 12 can drop below the sediment load at very low annual precipitation (a) or very fast erosion
 13 (c).
 14



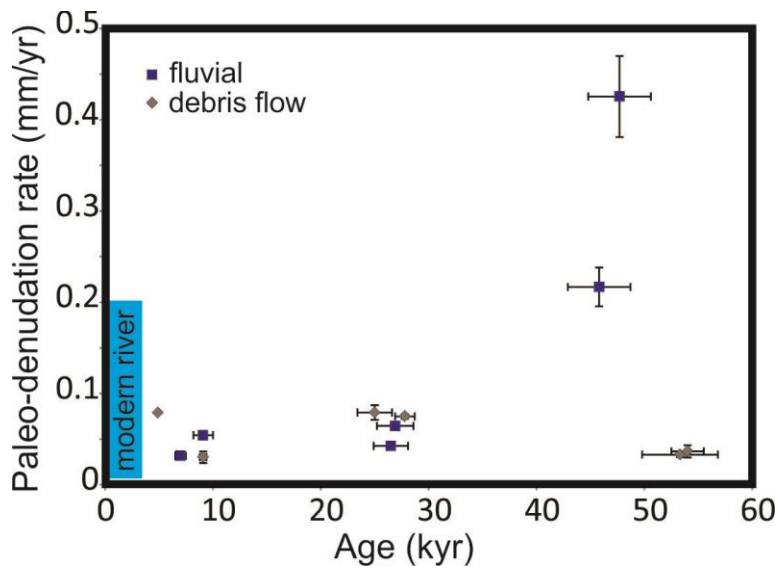
1

2

3 Figure 10. Model of hillslope erosion through (a) steady state erosion and (b) transient
 4 hillslope stripping. In each graph, the solid grey area indicates the range of the modern
 5 bedrock/alluvial transition. The cross-hatched area indicates the endmember locations of the
 6 bedrock/alluvial transitions for each scenario. The grey stippled lines indicate the location of
 7 the Pisco River terraces. In the steady state case, the sediment load, Q_s , is proportional to the
 8 aerially summed upstream denudation rate, D , even if there is a thick regolith mantle, h . The
 9 result is a minimal shift in the bedrock/alluvial transition (the point at which sediment load
 10 exceeds sediment transport capacity; *Tucker and Slingerland, 1997*) between wet and dry
 11 phases (b). In the transient case, the entire modelled soil mantle (after *Norton et al., 2014*) is
 12 stripped during a wet phase such that the sediment load, Q_s , is proportional to the aerially
 13 summed upstream regolith mantle, H , followed by a lack of sediment during the starved
 14 phase. The modelled result is a significant downstream shift in the bedrock/alluvial transition
 15 (c), which roughly corresponds to the observed occurrence of terraces in the Pisco valley.

16

17



1

2

3 Figure 11. Accelerated erosion following initial deposition of debris flow material supports
 4 the idea of rapid stripping of a stable regolith mantle. The initial high concentrations (low
 5 paleo-denudation rates) for the debris flow deposits could represent long residence time on
 6 hillslopes while the low concentrations (high paleo-denudation rates) for the fluvial material
 7 could be the result of rapid removal of the regolith cover (data after *Abbühl et al., 2011* and
 8 *Bekaddour et al., 2014*).